

A Stereoscopic Fibroscope for Camera Motion and 3D Depth Recovery during Minimally Invasive Surgery

David P. Noonan, Peter Mountney, Daniel S. Elson, Ara Darzi and Guang-Zhong Yang

Abstract— This paper introduces a stereoscopic fibroscope imaging system for Minimally Invasive Surgery (MIS) and examines the feasibility of utilizing images transmitted from the distal fibroscope tip to a proximally mounted CCD camera to recover both camera motion and 3D scene information. Fibre image guides facilitate instrument miniaturization and have the advantage of being more easily integrated with articulated robotic instruments. In this paper, twin 10,000 pixel coherent fibre bundles (590µm diameter) have been integrated into a bespoke laparoscopic imaging instrument. Images captured by the system have been used to build a 3D map of the environment and reconstruct the laparoscope's 3D pose and motion using a SLAM algorithm. Detailed phantom validation of the system demonstrates its practical value and potential for flexible MIS instrument integration due to the small footprint and flexible nature of the fibre image guides.

I. INTRODUCTION

AS the number of Minimally Invasive Surgical (MIS) procedures performed with robotic assistance multiplies, there is an increasing demand to improve the functionality and usability of such systems to allow for more complex procedures to be performed. Existing robotic assisted MIS platforms, such as the daVinci surgical robot (Intuitive Surgical, Sunnyvale, CA), allow a surgeon to interact with the operative environment through a master-slave architecture while viewing a magnified 3D representation of the surgical scene. The provision of immersive stereo vision has proved to be one of the major strengths of the system when manipulating complex anatomical structures.

Currently, one of the main focuses of MIS robot research is in the design of flexible instruments that can follow curved anatomical pathways with stereo vision, allowing regional and global integration of the 3D surgical environment. While traditional stereo-laparoscope systems, similar to that utilised by the daVinci, are not compatible with such an approach (due to the use of rigid, rod lens for the optical systems), miniaturised coherent fibre-optic bundles offer the advantages of flexibility and miniaturization required for integration with articulated instruments, but at a cost of decreased image resolution.

The purpose of this paper is to present a stereo imaging instrument to evaluate the feasibility of using fibre bundles for instrument localisation and soft tissue mapping within a

sequential vision only SLAM (Simultaneous Localisation and Mapping) system. Key technical issues associated with developing the stereo fibroscope imaging system and its 3D vision algorithms are presented. Such a system has the potential to provide *in situ* 3D reconstruction required for implementing advanced safety techniques, such as active constraints and motion stabilisation. Results obtained from a silicone tissue phantom and *ex-vivo* porcine tissue were validated using optical tracking and a registered CT scan.

A. Robotic Assisted Minimally Invasive Surgery

In MIS, a miniaturised CCD or fibre optic camera is commonly used to pass through a natural orifice or small incision of the body to gain remote vision. Specialised instruments are also inserted through additional incisions to perform the actual surgical tasks. The use of small incisions results in reduced patient trauma, blood loss and hospitalisation costs [1], thus making it an attractive alternative to open surgery. However, while procedures completed in this manner offer several advantages, the inherent technical difficulty is significantly higher as the distal dexterity is severely impaired by the long, rigid instruments and gross movements are subject to a fulcrum effect at the trocar port [2], as is illustrated in Fig. 1. Ergonomically, the visualisation provided is misaligned with the motor axis and is often through a monoscopic display, which lacks depth perception. This often leads to fatigue, poor hand-eye coordination and increased surgical errors [3].

Clinically, several robotic platforms have been developed to overcome these difficulties. The daVinci surgical robot, for example, operates as a tele-manipulator, where the surgeon controls miniaturized slave instruments on three or four robotic arms via a master console [4]. The system successfully tackles some of the traditional difficulties associated with MIS by providing stereoscopic visualisation, an ergonomic seating position, improved distal dexterity, motion scaling and tremor filtering at 6Hz.

In order to operate along curved anatomical pathways and access regions which are not in a direct line of sight from the incision point, there is currently increasing research interest into the development of flexible or articulated robotic systems. Example systems include the *Highly Articulated Robotic Probe (HARP)* for epicardial atrial ablation [5], a “snake” like robotic system designed to provide additional dexterity at the instrument tip for Ear, Nose and Throat (ENT) surgery [6], and a high-dexterity, modular instrument for coronary artery bypass grafting [7]. Systems with alternative white light and fluorescence imaging [8] have also been proposed. A natural extension of such systems is

Manuscript received September 15, 2008.

D. Noonan, P. Mountney, D. Elson, A. Darzi, G-Z. Yang are with the Institute of Biomedical Engineering, Dept. of Biosurgery & Surgical Technology, Dept. of Computing, Imperial College London, London, SW7 2AZ, UK (e-mail: g.z.yang@imperial.ac.uk).

the provision of camera position with simultaneous 3D scene reconstruction through stereo vision so that advanced functions such as adaptive motion stabilisation, augmented reality, active constraints and dynamic view expansion can be deployed [9] [10] [11]. The stereo fibre image guide based system described in this paper is ideally placed for integration with such flexible systems where miniaturization is a key requirement.

B. Simultaneous Localization and Mapping (SLAM)

Estimating the position of a camera relative to its environment and a 3D model of that environment is an important and challenging problem in robotic vision. The ability of SLAM to build long term maps and remain robust to drift has led to the development of many systems using a variety of hardware from ultrasound to laser range finders and cameras. The majority of these systems have been developed for mobile robots navigating in urban environments, and the size of the hardware is not compatible with robotic assisted surgery. It has been shown that optical approaches can be used to recover 3D structure in MIS [10, 11]. Such approaches are non invasive and make use of hardware which is already available during surgery. However, these methods face a number of challenges due to the complexity of the environment. 1) Features on the surface of tissue may be sparse and change in appearance as the anatomical feature may be below the surface. 2) Specular highlights need to be detected and ignored, they may also occlude features. 3) The lighting conditions can vary significantly, changing the appearance of features. 4) Tissue is not rigid and can deform as a result of respiration, cardiac motion and tissue tool interaction.

The use of miniaturised fibre bundles introduces additional challenges in the form of image resolution. Pixel count is compromised for a reduction in bend radius of the fibre bundles, thus leading to low quality images. Additionally, SLAM is made more challenging due to the small baseline between the stereo pair and the short working distance and limited field-of-view of the GRIN lens, which is used to focus the light into the bundles.

In [12], we demonstrated the principal that SLAM could be used in MIS with high quality stereo cameras in a rigid laparoscope. In [13], a monocular SLAM system is presented for ENT surgery, however the environment mapped is small and features appear to be in the scene the entire time and no loops are closed. A system developed by [11] is used to map larger areas however the approach relies on the use of an Optotrak to track the laparoscope making the assumption that the scope is rigid.

While the previous work utilized the high quality images captured using the stereo laparoscope of the daVinci system, an equivalent image resolution and field-of-view is not currently available with flexible fibre image guides. As such the system described in this paper was developed to identify and overcome technical difficulties from mechanical, calibration and software algorithm perspectives, in order to evaluate the feasibility of accurate camera localisation and tissue mapping.

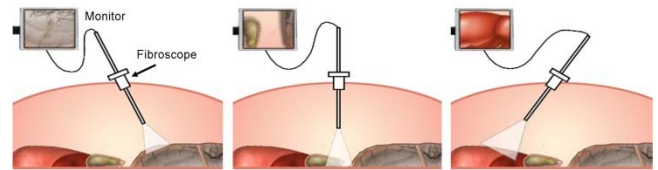


Figure 1: Schematic illustration of a typical endoscope motion *in-vivo*.

II. EXPERIMENTAL SETUP

A. Mechanical & Optical System Design

The stereo video sequences used in this paper were recorded using free-hand data acquisition with a custom stereo fibroscope test-rig as shown in Fig. 2. The system was designed to allow for the acquisition of stereo images using fibre image guides and to facilitate the validation of the algorithms which were then experimentally tested on the resulting images.

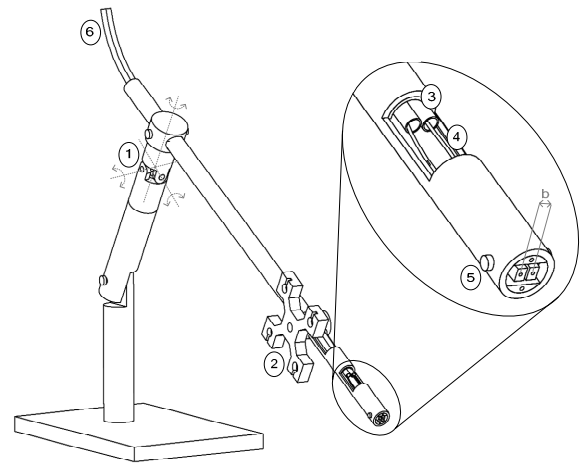


Figure 2: Schematic illustration of the stereo fibroscope indicating the location of 1) 3-axis joint to allow for free-hand camera motion, 2) Rigid body to mount optical tracking markers to provide ground truth data for camera motion validation, 3) Protective tubing for fibre bundles 4) 10,000 pixel coherent fibre image guide (x2) 5) Grub screw (x2) to adjust camera vergence and 6) Tubing path to image acquisition system. The camera baseline, b , of 3.8mm is also marked.

The system features stereo flexible, coherent fibre image guides (Sumitomo IGN-05/10, 10,000 fibres, length 1.5 m, diameter 0.59mm, min. bend radius 25mm) running down a rigid shaft of diameter 10mm in a configuration similar to a laparoscope. The fibres, (4) in Fig. 2, are housed in twin protective polyurethane sheaths (3) which are clamped both within the shaft and just prior to an optical mounting stage. The fibres exit the sheaths and are clamped into place before passing through twin adjustable distal tip mounting arms. The separation of the arms (and thus the distance between the fibres) can be adjusted using grub screws threaded through the aluminium outer casing of the shaft (5). This allows the baseline, b , and vergence of the stereo pair to be adjusted as required. The baseline used during the experiments described in this paper was 3.8mm. A graded index (GRIN) lens (Grintech GmbH) is cemented onto the end of each image guide (diameter 0.5mm, working distance 10mm, NA 0.5) to image an area of $35 \times 35 \text{ mm}^2$ at a working distance of 20mm onto the distal end of each image guide.

The fibres are both clamped into a single fibre mount and imaged onto a CCD camera (UEye, UI-2250-C/CM) using an achromatic $\times 10$ microscope objective and 100mm focal length lens, as shown in Fig. 3.

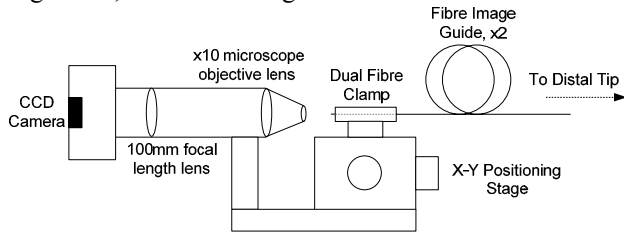


Figure 3: Schematic illustration of the optical setup. The flexible image guides are housed in a custom clamp attached to an XY positioning stage. This allows for fine focussing of the images onto the objective lens and thus the CCD. Both left and right images are captured on one CCD and segmented offline.

Focussing of the fibres is performed by adjusting the position of the fibre mount. This is achieved with micrometre precision using an XY positioning stage. The fibre bundles are pivoted around a point 315mm from their distal tips (close to the first image plane) to allow free-hand rotations in a manner similar to a laparoscope passing through a trocar port.

For validation, a removable rigid body with four optical tracking markers was attached 117mm from the distal tip of the fibroscope. This aspect of the system will be further discussed in Section III.

The following calibration steps were then required to allow for data acquisition:

- The orientation of the camera co-ordinate system in the left camera image was defined manually to account for the arbitrary rotation about the camera co-ordinate system's z -axis which occurs due to the rotation of the fibre bundle between its two clamping points
- To account for this same arbitrary rotation about the z -axis in the right image, its camera co-ordinate system was calibrated to co-align with that of the left image
- Stereo camera calibration was performed to calculate the intrinsic and extrinsic parameters and to correct for non-linear radial lens distortion [14]. This step was performed manually due to the low resolution causing failure of the automatic corner detection
- A hand-eye calibration to compute the relative rotation and translation from the rigid body to the left camera centre was then performed using the technique proposed by Tsai and Lenz [15].

Example stereo images taken with the system on both an *ex-vivo* porcine tissue sample and a silicone soft tissue phantom are shown in Fig. 4. The completed system, showing the fibroscope, rigid body and the optical system, is depicted in Fig. 5.

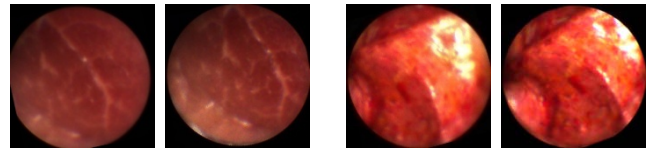


Figure 4: Sample images captured with the stereo fibroscope of *ex-vivo* porcine tissue (left) and a silicone soft tissue phantom (right).

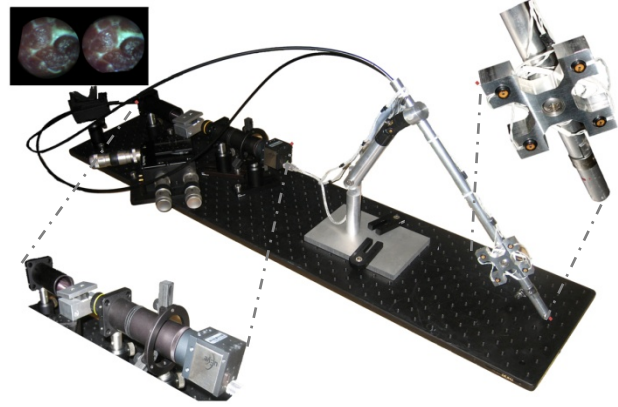


Figure 5: Image showing the complete system. The optical setup including fibre mount, objective lens and camera is shown on the lower left. The rigid body used for validation purposes is shown in the top right.

B. SLAM Algorithm Design

A SLAM approach was adopted using an Extended Kalman Filter system and stereo images giving 6DOF SLAM similar to [12]. A “constant velocity, constant angular velocity” motion model is used with a deterministic and a stochastic element to model unknown user motion.

1) Map management

The type of tissue or organ, distance between camera and tissue and the illumination all affect the visual appearance of the tissue. This problem is exacerbated by the limited resolution of fibrosopes. To cope with this challenging environment and improve runtime performance a sparse feature map is used tracking up to 20 features at a time. Features are detected using a Difference of Gaussian detector, matched in the right and left image by searching along the epipolar line and using a normalized cross correlation. Outliers were removed using RANSAC. The features were triangulated to estimate their 3D position relative to the camera. This position was then reprojected into the image plane and features with a large reprojection error were rejected. In initial experiments we found that due to the visual appearance of tissue the features clustered around one or two regions in the image leading to poor quality maps making accurate localization difficult. It has been shown [16] that using a fish eye lens to increase the field of view can improve SLAM, however here we are limited to a small field-of-view and short working distance, making feature selection and map management more important. Ideally we want to observe the same features for as long as possible in order to reduce uncertainty in the features 3D position. We found the best approach to this problem was to use features close to the edge of the image. Although this makes map building and localisation more robust, changes in illumination alter the appearance of features making tracking more challenging. Specular highlights can cause significant problems during tracking in

a MIS environment. Specular highlights in the images were detected using a manually defined threshold in the HSV colour space.

2) 3D Surface reconstruction

The solid surface representation is generated by performing Delaunay triangulation on the SLAM map. This meshing approach provides an estimate for every 3D point within the observed and mapped environment. The mesh is textured with images taken from the left fibroscope to build up a realistic representation of the environment. Image rectification is performed before the textures are applied to the mesh in order to remove distortion. To improve the visual appearance of the 3D reconstruction we search for images which cover the largest number of points in the map in order to generate models which are more consistent.

3) Honeycomb artifact removal

The light directed down the two image guides of the fibroscope is captured by a distal CCD camera. As a result, the structure of the individual fibres is visible in the image as a honey comb structure (see Fig. 6), which can adversely effect feature detection and tracking. Several different approaches have been proposed for removal of the honeycomb effect or defocusing the proximal imaging optics, including estimations based on Bayer CCD patterns and shaped Fourier filters [17] aimed at estimating the honey comb structure.

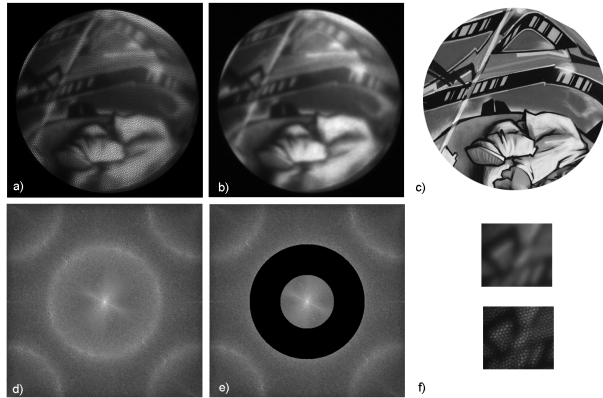


Figure 6: a) Original test image captured by fibre bundle b) Test image after honeycomb removal c) Original test image d) Fourier of original image e) band pass filter applied in Fourier domain f - top) close up of (b); f- bottom) close up of (a)

During the experiments, we found that sub-millimetre movements of the optics relative to the CCD could lead to changes in the image and movement of the honeycomb structure on the CCD chip. As we could not rely on the honeycomb structure being static relative to the camera we needed a reliable and robust approach which did not need recalibrating each time the system is used. We found that sufficient image restoration for tracking could be achieved using a band pass filter [18] in the Fourier frequency space followed by Gaussian smoothing. This successfully removed the structure in the image without affecting the performance of the tracker.

4) Feature tracking

Tracking tissue features is challenging as they may be sparse, varying with different lighting conditions and

affected by specular highlights. Furthermore, the images acquired by the proposed system are low in resolution due to the limited number of fibres used. The intensity of the light transmitted by the fibre bundles can vary leading to changes in the visual appearance of features. To cope with this environment a feature tracking system similar to [19] was used in an active search context. This approach adapts to the image content learning features online and directly from the image space. The method is particularly suitable for MIS images where features appear similar and may not be globally distinctive. This approach learns the most discriminative information for feature tracking, allowing it to robustly track locally unique features. The approach has been extended in this paper to include synthetically generated data. Synthetic data is generated by warping the image patch around the detected feature with an affine transformation in order to make the feature tracking more robust and able to track reliably from a single learning frame. This is important for fiberoptic images because the field of view is small and features may only appear for a short period of time.

III. VALIDATION SETUP

A. Camera Motion Ground Truth Acquisition

In order to validate the accuracy of the camera motion as reconstructed by the SLAM algorithm, a rigid body was attached approximately 117mm from the distal tip of the stereo fibroscope using four optical tracking markers (Northern Digital Inc, Ontario, Canada). A Rigid Body co-ordinate system ($C_{RigidBody}$) was defined at the origin of the four markers. The position and orientation of this system with respect to the World co-ordinate system (C_{World}) is known at all instances in time. The measured rotations and translations of this rigid body w.r.t. the world co-ordinate system were transformed to the camera co-ordinate system using the following transformation:

$${}^{cc}T = {}^{cc}T {}^{rb}T {}^wT$$

Where:

${}^{rb}T {}^wT$ is provided by the optical tracker.

${}^{cc}T {}^{rb}T$ is obtained using a Hand-Eye transformation from the origin of C_{RB} to the camera centre of the left fibre bundle, ${}^{RB}T {}^{cc}T$. This was performed using techniques similar to [15].

B. 3D Model Validation

To validate the SLAM algorithm, a silicone soft tissue phantom was constructed and latex paints were used to simulate specular reflections. A Computed Tomography (CT) scan of the phantom was performed in order to provide ground truth. Prior to scanning, the model was embedded with CT visible markers which were easily identifiable in the resulting scan. During the data acquisition phase of the experiment the location of each of the markers was identified using a stylus which contained a second rigid body of four optical tracking markers with a co-ordinate system C_{stylus} . This allowed for each of the markers to be identified

with respect to the world co-ordinate system and thus the camera co-ordinate system.

A comparison between the surface of the CT reconstruction and the point map generated by the SLAM algorithm was performed. This required a process to find points on the surface of the CT which corresponded to the 3D features in the SLAM map. Features detected in the image were projected into the registered CT model from the camera's position given by the Optotrak. The projected ray was traced through the 3D CT model to detect the first plane it intersects. This point is taken to be the corresponding point in the CT surface.

IV. RESULTS

A. Camera Motion

Fig. 7 shows four reconstructed surfaces from the video sequence. The blue line represents the ground truth camera trajectory and the green line represents the trajectory reconstructed by the SLAM algorithm. The stereo fibroscope was moved by hand to explore unknown regions of the phantom and to close a loop. It can be seen that the loop was successfully closed. As the fibroscope moves into unknown regions towards the end of the trajectory, an error propagation leads to a small amount of drift being introduced to the position estimate. This in part can be attributed to the low resolution of the camera limiting the 3D reconstruction and tracking accuracy.

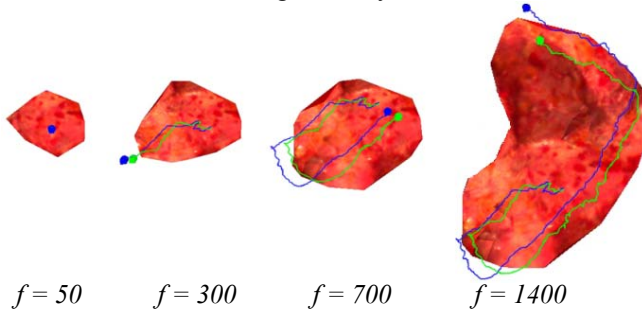


Figure 7: Ground truth camera trajectory (blue) and SLAM reconstructed camera trajectory (green) at four different frame intervals

Fig. 8 illustrates the trajectories when decomposed into motions along the x , y and z axes for 1400 frames. The absolute error in the three different axes was 1.94mm, 0.7mm and 1.7mm respectively. There was no rotation around the z axis and only a minimal amount of rotation around the x and y axes.

An additional *ex-vivo* experiment was carried out using excised porcine tissue. The camera was moved in a motion in which to close a loop and continue to explore in a similar manner to the phantom experiment. As shown in Fig. 9, the loop was successfully closed by the SLAM algorithm.

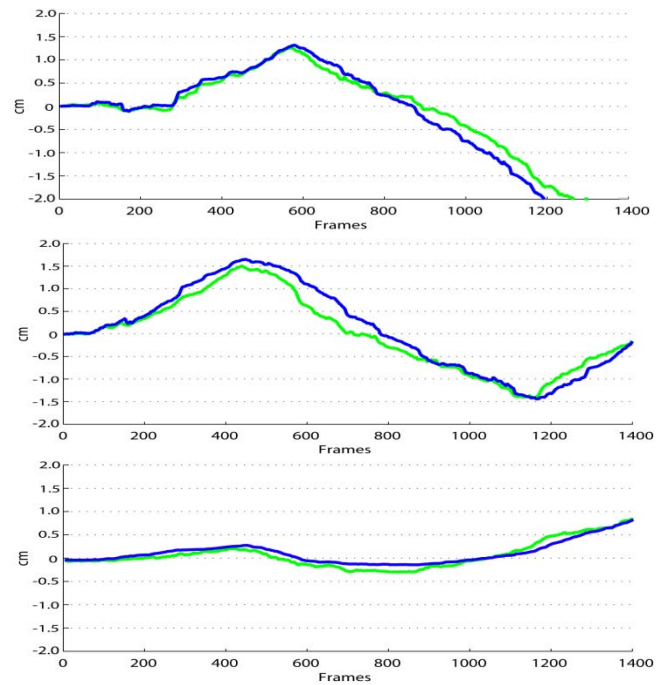


Figure 8: Trajectories decomposed into individual X, Y and Z components. The ground truth from optical tracking markers is shown in blue and the motion as reconstructed by the SLAM algorithm is shown in green

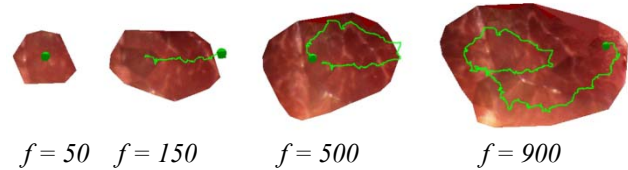


Figure 9: Reconstructed 3D surface and camera motion as generated by the SLAM on an *ex-vivo* porcine tissue sample.

B. Surface Reconstruction

Fig. 10 illustrates the 3D surface generated by the SLAM algorithm (*right*) alongside the ground truth 3D surface extracted from the CT scan of the phantom (*left*) from three different views. It can be seen that the scale, orientation and geometry of the surfaces are visually similar. Local differences in geometry can be attributed to the sparseness of the SLAM map. Due to the meshing of the sparse map, which fits planes between points, the recovered surface is likely to be less accurate at representing local changes in geometry. The overall reconstruction errors for the surface for x , y and z are 2mm, 1.3mm and 2.9mm respectively. The surface was approximately 35mm from the camera position during the data capture. The reconstruction error is larger in the z axis as expected since the resolution of the images and small baseline between the fibre image guides makes stereo triangulation less accurate.

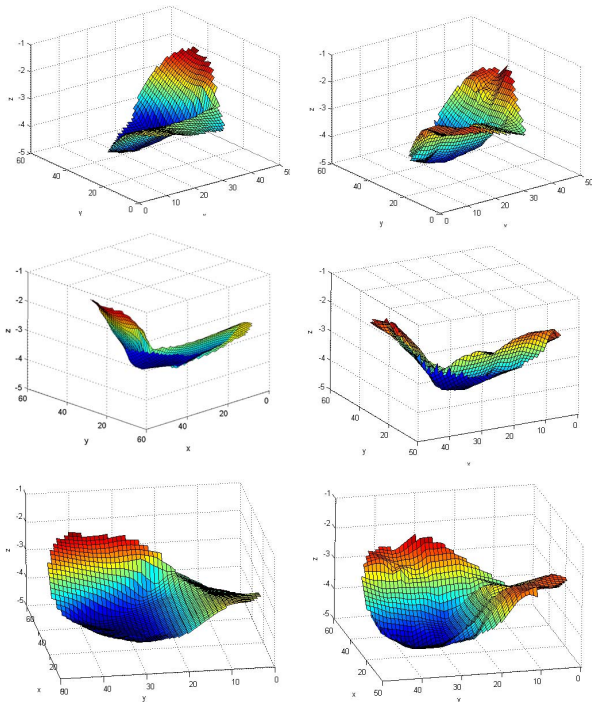


Figure 10: Reconstructed 3D surface as generated by the SLAM (right) and co-registered CT ground truth data (left)

V. CONCLUSION

The paper demonstrates the feasibility of integrating twin flexible fibre image guides in a stereo configuration to capture images in an MIS environment. The challenges overcome to construct and calibrate this bespoke image system, along with image enhancement and robust feature tracking techniques are presented. The resulting images were successfully employed by a SLAM algorithm to both track camera pose and motion and generate a 3D model of the environment. It was anticipated that the limited resolution offered by coherent fibre bundles might make this approach infeasible. However, although the image resolution does affect the final results, they clearly demonstrate that such an approach is possible.

One of the limitations of a feature based optical approach is that it can be affected by the paucity of tissue surface features. One potential solution is to use structured light. The sparse map limits the 3D model reconstruction accuracy. This information could be improved by including dense reconstruction information or combining it with other approaches such as shape from shading. The next major challenge to address for this system is that of tissue deformation. Deformation occurs due to tool-interaction, respiration and cardiac induced tissue motion. This can violate the static world assumption made by SLAM. Although the current system can cope with a very small amount of deformation, as this increases the 3D map will be inaccurate because it does not represent the deformation and the fibroscope position estimate will be less accurate. One potential application of the proposed framework is within a catheter which utilizes the stereo vision for targeting and depth information for accurate focused energy delivery.

ACKNOWLEDGMENT

The authors would like to thank the Hamlyn Centre for Robotic Surgery for funding this proof-of-concept study and Drs Andrew Davison, Danail Stoyanov and Phillip Edwards for their support and advice.

REFERENCES

- [1] K. H. Fuchs, "Minimally Invasive Surgery," *Endoscopy*, vol. 34, pp. 154-159, 2002.
- [2] I. Crothers, A. Gallagher, N. McClure, D.T.D. James, and J. McGuigan, "Experienced laparoscopic surgeons are automated to the "fulcrum effect": an ergonomic demonstration," *Endoscopy*, vol. 318, pp. 365-369, 1999.
- [3] O. Elhage, D. Murphy, B. Challacombe, A. Shortland, and P. Dasgupta, "Ergonomics in Minimally Invasive Surgery," *International Journal of Clinical Practice*, vol. 61, pp. 181-188, 2007.
- [4] P. Dario, B. Hannaford, and A. Menciassi, "Smart Surgical Tools and Augmenting Devices," *IEEE Transactions on Robotics and Automation*, vol. 19, pp. 782-792, 2003.
- [5] T. Ota, A. Degani, B. Zubiate, A. Wolf, H. Choset, D. Schwartzman, and M. Zenati, "Epicardial Atrial Ablation Using a Novel Articulated Robotic Medical Probe Via a Percutaneous Subxiphoid Approach," *Innovations: Technology & Techniques in Cardiothoracic & Vascular Surgery*, vol. 1, pp. 335-340, 2006.
- [6] N. Simaan, R. Taylor, and P. Flint, "A Dexterous System for Laryngeal Surgery," in *International Conference on Robotics and Automation*, 2004, pp. 351-357.
- [7] D. Salle, P. Bidaud, and G. Morel, "Optimal Design of High Dexterity Modular MIS Instrument for Coronary Artery Bypass Grafting," in *IEEE International Conference on Robotics and Automation*, 2004, pp. 1276-1281.
- [8] D. P. Noonan, D. Elson, G. Mylonas, A. Darzi, and G.-Z. Yang, "Laser Induced Fluorescence and Reflected White Light Imaging for Robot-Assisted Minimally Invasive Surgery," *IEEE Transactions on Biomedical Engineering*, 2008. In Press.
- [9] G. Mylonas, K.-W. Kwok, A. Darzi, and G.-Z. Yang, "Gaze-Contingent Motor Channelling and Haptic Constraints for Minimally Invasive Robotic Surgery," in *MICCAI*, 2008, pp. 347-355.
- [10] D. Stoyanov, A. Darzi, and G.-Z. Yang, "Dense 3D Depth Recovery for Soft Tissue Deformation During Robotically Assisted Laparoscopic Surgery," in *MICCAI*, 2004, pp. 41-48.
- [11] C. Wengert, L. Bossard, A. Haberling, C. Baur, G. Szekely, and P. C. Cattin, "Endoscopic Navigation for Minimally Invasive Suturing," in *MICCAI*, 2007, pp. 620-627.
- [12] P. Mountney, D. Stoyanov, A. Davison, and G.-Z. Yang, "Simultaneous Stereoscopic Localization and Soft-Tissue Mapping for Minimal Invasive Surgery," in *MICCAI*, 2006, pp. 347-354.
- [13] D. Burschka, M. Li, M. Ishii, R. H. Taylor, and G. D. Hager, "Scale-invariant registration of monocular endoscopic images to CT-scans for sinus surgery," in *MICCAI*, 2004, pp. 413-426.
- [14] Z. Zhang, "A Flexible New Technique for Camera Calibration," *IEEE Transactions on Pattern Analysis and Machine Intelligence*, vol. 22, p. 1330-1334, 2000.
- [15] R. Tsai and R. Lenz, "Real Time Versatile Robotic Hand/Eye Calibration using 3D Machine Vision," in *IEEE International Conference on Robotics and Automation*, 1988, pp. 554-561.
- [16] A. J. Davison, Y. G. Cid, and N.Kita, "Real-Time 3D SLAM with Wide-Angle Vision" in *IFAC Symposium on Intelligent Autonomous Vehicles*, 2004.
- [17] C. Winter, S. Rupp, M. Elter, C. Munzenmayer, H. Gerhauser, and T. Wittenberg, "Automatic adaptive enhancement for images obtained with fiberoptic endoscopes," *IEEE Transactions on Biomedical Engineering*, vol. 53, pp. 2035-2046, 2006.
- [18] M. M. Dickens, D. J. Bornhop, and S. Mitra, "Removal of Optical Fiber Interference in Color Micro-Endoscopic Images," in *11th IEEE Symposium on Computer Based Medical Systems*, 1998, p. 246.
- [19] P. Mountney and G.-Z. Yang, "Soft Tissue Tracking for Minimally Invasive Surgery: Learning Local Deformation Online," in *MICCAI*, 2008, pp. 364-372.